

Theory for the Solubility of Gases in Polymers: Application to Monatomic Solutes

John G. Curro*

Sandia National Laboratories, Albuquerque, New Mexico 87185

Kevin G. Honnell

Los Alamos National Laboratory, Los Alamos, New Mexico 87545

John D. McCoy

Department of Materials & Metallurgical Engineering, New Mexico Institute of Mining & Technology, Socorro, New Mexico 87801

Received July 23, 1996; Revised Manuscript Received October 24, 1996[®]

ABSTRACT: The polymer reference interaction site model (PRISM theory) is applied to the problem of calculating the solubility of monatomic gases in amorphous polyethylene. One can consider this system as an approximation to the solubility of gases in ethylene/propylene elastomers. The chemical potential of a solute atom in the polymer is decomposed into two distinct contributions: a positive athermal contribution calculated by growing the solute atom from a point particle and a negative attractive contribution computed from first-order perturbation theory using the athermal system as the reference state. Good agreement is found between the PRISM calculations and available experimental data on solubility of gases in common elastomers with no adjustable parameters. Furthermore, PRISM theory is successful in predicting several interesting trends observed experimentally: (1) solubility increases with the size of the solute atom, (2) solubility is a monotonically increasing function of the critical temperature of the solute species, and (3) the temperature coefficient of solubility crosses over from positive to negative for solutes having critical temperatures of approximately 65 K.

I. Introduction

The sorption of gases in polymers is important in numerous applications, particularly where gas permeability plays an important role. Since the permeability coefficient is the product of the solubility and the diffusion constant, gas sorption is crucial in applications such as gas separation membranes, diffusion barrier materials, polymer foaming processes, and plasticization. Furthermore, O₂ permeability can be the rate-determining factor controlling polymer degradation processes such as oxidation.¹ The purpose of the present investigation is to apply recent integral equation theories of polymers to the problem of calculating the solubility of gases as a function of polymer architecture and solute species.

In our initial application presented here, we will confine ourselves to amorphous polymers at equilibrium above their glass transition temperature. This could include polymer liquids or cross-linked elastomers. Furthermore, we will focus on the Henry's law regime, where the solubility is low; generalization to higher solubility is straightforward. Previous workers^{2,3} applied the well-known Flory–Huggins theory⁴ to this problem. The Flory–Huggins theory reproduces qualitative features such as the shape of the adsorption isotherm. Good fits to experimental solubility data at a given temperature can be achieved by the proper choice of an empirical Flory–Huggins χ parameter. However, the Flory–Huggins theory suffers from several well-known deficiencies^{5,6} which limit its usefulness as a predictive tool. Since it is a lattice model, the

theory cannot capture the effects of solute and/or monomer size and shape on the solubility. Moreover, the Flory–Huggins theory assumes random mixing of monomers and, therefore, neglects the effect of polymer chain architecture on the intermolecular packing.

Polymer reference interaction site theory^{5,6} (polymer RISM or PRISM theory) has been successful in describing the structure and thermodynamics of polymer melts and alloys. Here we will apply the PRISM theory of Curro and Schweizer to the sorption of low molecular weight, single site solutes in polymers. Polymer RISM theory extends to polymers the ideas developed earlier by Chandler and Andersen^{7,8} in the RISM theory of molecular liquids. In order to compute the sorption of a gas in a polymer liquid, we require the chemical potential μ_A of the solute species A in the polymer. μ_A can be related to the pair correlations in the liquid following the work of Pratt and Chandler,^{8,9} who computed the Henry's law constant⁹ for methane in water.

As an illustration of the theory, we will consider the sorption of monatomic gases in a polyethylene melt as a function of temperature in the range 298–500 K. In reality, high-density polyethylene will crystallize¹⁰ below about 404 K; however, in our PRISM calculations we will maintain the polyethylene melt as amorphous below the experimental melting temperature. This hypothetical amorphous polyethylene should be a reasonable representation of the nearly amorphous, branched polyethylenes produced with metallocene catalysts, as well as ethylene propylene random copolymers at low propylene contents where the propylene moieties distributed randomly along the chain backbone preclude crystallization. Our motivation in this example calculation is to approximately model the solubility of gases in ethylene propylene rubber (EPR).

In this paper we will begin with a theoretical discussion aimed at calculating the chemical potential of a

* Author to whom correspondence should be addressed.

† Supported by the US Dept. of Energy under Contract number DE-AC04-94AL85000.

© Abstract published in *Advance ACS Abstracts*, January 1, 1997.

solute molecule in a polymer from polymer RISM theory. We then illustrate the method for the case of monatomic gases in polyethylene. Finally, comparisons will be made with experimental solubilities of a wide range of gases in various elastomers. We will show that PRISM theory successfully captures interesting general experimental trends regarding the temperature dependence of sorption and the scaling of solubility with the critical temperature of the solute species.

II. Theory

A. Flory–Huggins Theory. Previous workers^{2,3} have interpreted sorption data of gases in polymers using the Flory–Huggins theory.⁴ Using the Flory–Huggins expression for the free energy of mixing, it can be shown⁴ that the excess chemical potential $\Delta\mu_A$ of a solute A in a polymer B with N_B repeat units is given by

$$\Delta\mu_A = \ln \phi_A + \phi_B(1 - 1/N_B) + \chi\phi_B^2 \quad (1)$$

where ϕ is the volume (or site) fraction of A or B and χ is the Flory chi parameter. Due to the incompressibility assumption underlying the Flory–Huggins model, there is some ambiguity associated with the precise meaning of $\Delta\mu_A$. It is sometimes associated with the difference in chemical potentials between solvated species A and pure species A, either at the same temperature and pressure or, alternatively (and perhaps more rigorously), as the difference in solvated and pure chemical potentials at the same temperature and site density. For incompressible fluids the distinction is unimportant, as pressure does not enter as an independent variable; however, in applying eq 1 to real solutions the distinction, though presumably small, is real. For a cross-linked system Flory added⁴ an elastic free energy term important in swollen networks. Since our emphasis here is on the Henry's law regime, the volume change of the network due to the solute will not play an important role. We now equate the solute chemical potentials of the ideal gas and polymer phases at pressure P to obtain,

$$P = f_A^* \phi_A \exp[\phi_B(1 - 1/N_B) + \chi\phi_B^2] \quad (2)$$

with f_A^* being the fugacity of pure A at the temperature T and either pressure P or density ρ of the polymer, depending on the convention adopted in eq 1. For a condensable vapor at low to moderate pressure, the fugacity can be approximated by the vapor pressure. For a permanent gas, one could estimate f_A^* from the an equation-of-state or extrapolate from experimental data on pure A. At low pressures, we write Henry's law in the form

$$P = K_H \phi_A \quad \phi_A \rightarrow 0 \quad (3)$$

where K_H is the Henry's law constant dependent on temperature. We have defined Henry's law in eq 3 in terms of the site fraction rather than the conventional mole fraction definition to avoid the trivial dependence of K_H on the molecular weight of the polymer. From eq 2 we see immediately that the Henry's constant can be written as

$$K_H = f_A^* \exp(1 + \chi) \quad (4)$$

for high molecular weight polymers. Hence, there is a very simple relationship between the Henry's constant

and the well-known Flory chi parameter. However, since χ cannot normally be related to the interatomic potentials, eq 4 has limited predictive value.

B. PRISM Theory. In this investigation we will use the integral equation theory of molecular liquids to provide further insights into the sorption process. Here we employ polymer RISM or PRISM theory to describe the intermolecular packing between polymer chains and solute. Since it has been discussed in detail in previous papers^{5,6,11–18} we will only outline the essential elements of the approach. Consider a system containing small molecules of N_A sites in equilibrium with a polymer liquid having N_B repeat units per chain. Each repeat unit can contain one or more independent interaction sites. An interaction site can be a single atom or a small group of atoms making up the monomer structure. For example, we model polyethylene^{19,20} as consisting of N_B identical sites where each site represents a methylene group CH_2 . More complex monomer architectures can be built with additional independent sites.^{14,21} The intermolecular packing in such a system can be described in terms of intermolecular radial distribution functions $g_{\alpha\gamma}(r)$ defined as

$$\rho_\alpha \rho_\gamma g_{\alpha\gamma}(r) = \langle \sum_{i \neq j} \delta(\vec{r}_i^\alpha) \delta(\vec{r} - \vec{r}_j^\gamma) \rangle \quad (5)$$

where ρ_α is the site density of type α and \vec{r}_i^α is the position vector of site α on chain i . It should be emphasized that eq 5 averages over pairs of sites α and γ on different molecules. For polymers it is a good approximation to neglect chain end effects so that pair correlation functions are the same for any monomer along the chain backbone. For the case illustrated in this study of a monatomic gas in polyethylene, we have only two types of sites: site A, representing a solute atom, and site B, constituting a CH_2 group on the polyethylene backbone. Hence the intermolecular packing is characterized by three intermolecular radial distributions $g_{AA}(r)$, $g_{BB}(r)$, and $g_{AB}(r)$.

In PRISM theory^{5,6} we follow the work of Chandler and Andersen^{7,8} by defining an Ornstein–Zernike type of equation relating the radial distribution functions to the direct correlation functions. For convenience we write this generalized OZ equation in momentum space

$$\hat{H}_{\alpha\beta}(k) = \sum_{\sigma\lambda} \hat{\Omega}_{\alpha\sigma}(k) \hat{C}_{\sigma\lambda}(k) [\hat{\Omega}_{\lambda\beta}(k) + \hat{H}_{\lambda\beta}(k)] \quad (6)$$

where the carets denote Fourier transformation with respect to wave vector k . The functions $H_{\alpha\beta}(r)$ are the elements of a 2×2 (in this case) intermolecular total correlation function matrix defined according to

$$H_{\alpha\beta}(r) = \rho_\alpha \rho_\beta [g_{\alpha\beta}(r) - 1] \quad (7)$$

Likewise the functions $\Omega_{\alpha\beta}(r)$ represent the intramolecular structure functions defined as

$$\Omega_{\alpha\beta}(r) = \frac{\delta_{\alpha\beta} \rho_\alpha}{N_\alpha} \sum_{ij} \omega_{ij}(r) \quad (8)$$

with $\omega_{ij}(r)$ being the normalized probability density between i and j sites on a single chain or molecule of type α , and $\delta_{\alpha\beta}$ is the Kronecker delta.

The $C_{\alpha\gamma}(r)$ functions are the direct correlation functions and can be viewed as being defined by eq 6. To be able to solve for the intermolecular pair correlation functions, another set of relations or "closure" conditions

between $g_{\alpha\beta}(r)$ and $C_{\alpha\beta}(r)$ is required. Taking the approach of Chandler and Andersen,^{7,8} we approximate the direct correlation functions by the Percus–Yevick theory (PY) of atomic liquids.²² For hard-core potentials, the PY closure has the following simple form

$$g_{\alpha\beta}(r) = 0 \quad \text{for } r < d_{\alpha\beta} \quad (9a)$$

$$C_{\alpha\beta}(r) \cong 0 \quad \text{for } r > d_{\alpha\beta} \quad (9b)$$

where $d_{\alpha\beta}$ is effective hard-core distance between the α and β types of sites. Equation 9a is exact for hard-core potentials whereas eq 9b is an approximation making use of the fact that the direct correlation functions are typically short range functions of r at liquidlike densities.

The intramolecular structure factors contain information about the architecture and local chemical structure of the polymer chains. In general, these functions should be determined self-consistently with the intermolecular structure. To a good approximation,^{5,6} we can avoid the difficult self-consistency calculation by making use of the Flory ideality hypothesis⁴ which argues that, in a polymer melt, long-range excluded volume forces are screened out. Thus one can calculate the intramolecular structure function $\hat{\Omega}_{BB}(k)$ for the polymer component from a separate, single chain calculation, where long-range repulsive interactions along the chain backbone are intentionally set to zero. Such a calculation was performed earlier by Honnell and coworkers^{19,20,23} using a rotational isomeric state model for polyethylene. As in our earlier work, we divide the correlations along the chain backbone into short-range and long-range contributions by writing

$$\hat{\Omega}_{BB}(k) = \frac{\rho_B}{N_B} \sum_{\alpha} \left[\sum_{|\alpha-\beta| \leq 5} \omega_{\alpha\beta}(k) + \sum_{|\alpha-\beta| > 5} \omega_{\alpha\beta}(k) \right] \quad (10a)$$

The short-range term, in which $|\alpha - \gamma| \leq 5$, is evaluated rigorously by exact enumeration of the rotational isomeric states for the PE chain backbone. The long range term, for which $|\alpha - \gamma| > 5$, is estimated²³ from the “Koyama distribution” of a semiflexible chain where the second, $\langle r_{\alpha\beta}^2 \rangle$, and fourth moments, $\langle r_{\alpha\beta}^4 \rangle$, are chosen to match the complete rotational isomeric state model. Examples of the structure functions obtained for polyethylene macromolecules are shown in Kratky form in Figure 1 at three different temperatures. Notice that the value of the plateau (or intermediate scaling regime) on the y -axis decreases as the temperature is lowered, implying that the radius of gyration of polyethylene increases. This is a consequence of increased trans states along the chain backbone of polyethylene as the temperature is reduced.

For the case illustrated here, component A is simply a single site representing a monatomic gas atom, and the corresponding intramolecular structure function takes the simple form

$$\hat{\Omega}_{AA}(k) = \rho_A \quad (10b)$$

Generalization to other solutes containing more than one type of site is easily accomplished. Since the two sites A and B are on different molecules, the cross structure functions are zero, i.e., $\hat{\Omega}_{AB}(k) = 0$.

For given intramolecular structure factors, eqs 6, 7, and 9 can be solved numerically using standard Picard iteration methods.^{5,6} As an example, Figure 2 depicts

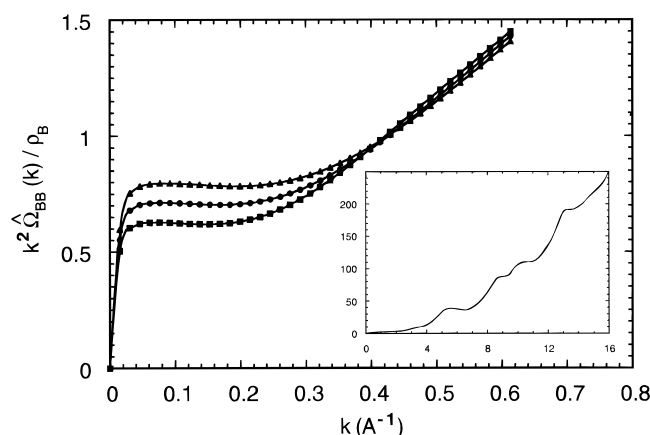


Figure 1. A Kratky plot of the intramolecular structure factor calculated for polyethylene ($N = 6429$) at three different temperatures: triangles, 298 K; circles, 400 K; squares, 500 K. The inset shows the behavior at higher wave vectors for the calculation at 400 K.

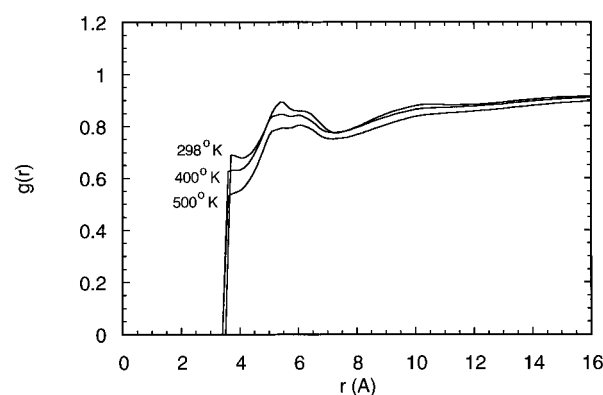


Figure 2. The intermolecular radial distribution function $g(r) \equiv g_{BB}(r)$ calculated from PRISM theory for methylene sites in polyethylene ($N = 6429$) melts at the three temperatures indicated.

the intermolecular radial distribution functions obtained for a pure, homopolymer melt of polyethylene chains at three different temperatures. Note that the intermolecular correlation functions exhibit system-specific packing features at short distances (< 10 Å), followed by a universal correlation hole regime where $g(r)$ approaches unity on a scale comparable to the radius of gyration of the chains.^{5,6} It has been demonstrated through extensive comparisons^{5,6} between PRISM theory, computer simulation, and wide angle X-ray scattering experiments that PRISM theory provides an accurate description of the intermolecular packing in polymer melts.

C. Athermal Chemical Potential. Consider first a two component, athermal reference system in which intermolecular sites of type α and γ ($=A$ or B) interact with purely repulsive, hard-core potentials $v_{\alpha\gamma}(r)$. The corresponding Mayer function can then be defined as

$$f_{\alpha\gamma}(r) = \exp[-\beta v_{\alpha\gamma}(r)] - 1 \quad (11a)$$

with $\beta \equiv 1/k_B T$. For hard-core potentials the Mayer functions become

$$\begin{aligned} f_{\alpha\gamma}(r) &= -1 & r < \frac{d_\alpha + d_\gamma}{2} \\ &= 0 & r > \frac{d_\alpha + d_\gamma}{2} \end{aligned} \quad (11b)$$

Following the work of Chandler,⁸ we define a charging parameter (λ) that grows the hard-core diameter (d_A) of a solute atom from a point, as λ varies between 0 and 1. The Mayer functions can then be viewed as functions of λ .

$$\begin{aligned} f_{AA}^{(\lambda)}(r) &= -1 & r < \lambda d_A \\ &= 0 & r > \lambda d_A \end{aligned} \quad (12a)$$

$$\begin{aligned} f_{AA}^{(\lambda)}(r) &= -1 & r < \frac{d_B + \lambda d_A}{2} \\ &= 0 & r > \frac{d_B + \lambda d_A}{2} \end{aligned} \quad (12b)$$

For this athermal system, Chandler⁸ has shown that the Helmholtz free energy (A_{ref}) can be written in the form

$$\frac{-2\beta(A_{\text{ref}} - A_0)}{V} = \int_0^1 d\lambda \int d\vec{r} \left[\rho_A^2 y_{AA}^{(\lambda)} \frac{df_{AA}^{(\lambda)}}{d\lambda} + 2\rho_A \rho_B y_{AB}^{(\lambda)} \frac{df_{AB}^{(\lambda)}}{d\lambda} \right] \quad (13)$$

In eq 13 we use the subscript ref to emphasize that we are considering the athermal mixture as our reference system. ρ_A and ρ_B are number densities of solute and B sites on the polymer, respectively, and the indirect correlation function is defined according to

$$y_{\alpha\gamma}^{(\lambda)}(r) = \exp[\beta v_{\alpha\gamma}(r)] g_{\alpha\gamma}^{(\lambda)}(r) \quad (14)$$

A_0 is then the corresponding Helmholtz free energy of an ideal gas of point solute particles in the polymer.

For the case under study we consider component A to be a single site, monatomic gas and component B to consist of the polymer. To calculate the solubility we require the chemical potential μ_A for inserting a gas molecule into the polymer.

$$\mu_A = \left[\frac{(\partial A/V)}{\partial \rho_A} \right]_{\rho_B} \quad (15)$$

From eq 13 we then obtain the chemical potential for the athermal reference system in the limit of low concentration of component A

$$\beta\mu_{\text{ref}} = \beta\mu_0 - 4\pi\rho_B \int_0^1 d\lambda \int_0^\infty r^2 dr y_{AB}^{(\lambda)}(r) \frac{df_{AB}^{(\lambda)}}{d\lambda} \quad (16)$$

μ_0 is the chemical potential for inserting a point particle into the polymer. Equation 16 can be simplified by recognizing that, for hard-core potentials,

$$\frac{\partial f_{AB}^{(\lambda)}}{\partial \lambda} = -\delta \left[r - \left(\frac{d_B + \lambda d_A}{2} \right) \right] \frac{d_A}{2} \quad (17)$$

where $\delta(r)$ is the Dirac delta function. By substituting eq 17 into eq 16 we can perform the inner integral to obtain

$$\beta\mu_{\text{ref}} = \beta\mu_0 + \frac{\pi d_A \rho_B}{2} \int_0^1 d\lambda (d_B + \lambda d_A)^2 y_{AB}^{(\lambda)} \left(\frac{d_B + \lambda d_A}{2} \right) \quad (18)$$

It can be seen from eq 14 that for hard-core potentials

$y_{AB}(d^+) = g_{AB}(d)$. This permits further simplification of eq 18:

$$\beta\mu_{\text{ref}} = \beta\mu_0 + \frac{\pi d_A \rho_B}{2} \int_0^1 d\lambda (d_B + \lambda d_A)^2 g_{AB}^{(\lambda)} \left(\frac{d_B + \lambda d_A}{2} \right) \quad (19)$$

Generalization of eq 19 to polymers in which the monomer contains more than one type of site is straightforward.

In this study we will treat the gas phase in equilibrium with the polymer as being an ideal gas of N_A atoms of mass m at pressure P . From the theory of perfect gases we can write the chemical potential μ_{ig} for inserting a solute atom into the gas as

$$\beta\mu_{\text{ig}} = \ln(\beta P \Lambda^3) \quad (20a)$$

where $\Lambda = h/\sqrt{2\pi m k_B T}$ and h is Planck's constant. μ_0 in eq 19 can be readily obtained by treating the point particles in the athermal polymer as an ideal gas of N_A atoms in the unoccupied polymer volume $V(1 - \eta)$, where η is the packing fraction of the liquid.

$$\beta\mu_0 = \ln[\rho_A \Lambda^3 / V(1 - \eta)] \quad (20b)$$

D. Enthalpic Chemical Potential. We now consider the effect of attractive interactions on the chemical potential. This can be accomplished using standard first-order perturbation theory of liquids²² with the athermal system as the reference state. For convenience we choose to represent the intersite potential $v_{\alpha\gamma}(r)$ as a Lennard–Jones potential

$$v_{\alpha\gamma}(r) = 4\epsilon [(\sigma_{\alpha\gamma}/r)^{12} - (\sigma_{\alpha\gamma}/r)^6] \quad (21)$$

In perturbation theory we divide the potential $v_{\alpha\gamma}(r) = u_{\alpha\gamma}(r) + w_{\alpha\gamma}(r)$ into a repulsive branch, $u_{\alpha\gamma}(r)$, and an attractive branch, $w_{\alpha\gamma}(r)$. For computational simplicity this decomposition of the potential is taken to be of the Barker–Henderson²⁴ type in which

$$\begin{aligned} u_{\alpha\gamma}(r) &= v_{\alpha\gamma}(r) & r \leq \sigma_{\alpha\gamma} \\ &= 0 & r > \sigma_{\alpha\gamma} \end{aligned} \quad (22a)$$

$$\begin{aligned} w_{\alpha\gamma}(r) &= 0 & r \leq \sigma_{\alpha\gamma} \\ &= v_{\alpha\gamma}(r) & r > \sigma_{\alpha\gamma} \end{aligned} \quad (22b)$$

It is well-established²² that, at high density, the structure or pair correlation functions $g_{\alpha\gamma}(r)$ are almost entirely determined by the repulsive part of the interactions. Hence we take our reference system to be the athermal problem discussed above. The attractive potential $\beta w_{\alpha\gamma}(r)$ is then treated perturbatively. To first-order we can then write^{22,24}

$$\frac{\beta A}{V} \cong \frac{\beta A_{\text{ref}}}{V} + \frac{\beta}{2} [\rho_A^2 \int_{\sigma_{AA}}^\infty w_{AA} g_{AA}^0 d\vec{r} + \rho_B^2 \int_{\sigma_{BB}}^\infty w_{BB} g_{BB}^0 d\vec{r} + 2\rho_A \rho_B \int_{\sigma_{AB}}^\infty w_{AB} g_{AB}^0 d\vec{r}] \quad (23)$$

in which the $g_{\alpha\gamma}^0(r)$ are determined from the athermal reference system. In this work we obtain these $g_{\alpha\gamma}^0(r)$ correlation functions from PRISM theory with purely hard-core repulsions for $r < d_{\alpha\gamma}$ between sites α and γ . For convenience, we employ the Barker–Henderson^{22,24}

Table 1. Lennard–Jones Parameters

site	σ (Å)	ϵ/k_B (K)	T_c (K)
He	2.57	10.8	5.1
Ne	2.75	35.8	44.3
Ar	3.41	119	151
Xe	4.07	225.3	289.6
CH ₂	3.905	59.4	

scheme to obtain the optimum hard-core diameter from the purely repulsive Lennard–Jones potential $u_{\alpha\gamma}(r)$ in eq 22a.

$$d_{\alpha\gamma} = \int_0^\infty \{1 - \exp[-\beta u_{\alpha\gamma}(r)]\} dr \quad (24)$$

The chemical potential can then be calculated by differentiation of eq 23.

E. Solubility and Henry's Law. The chemical potential μ_A^p of a solute A in the polymer phase, in the limit of low solubility, can now be expressed as

$$\mu_A^p = \mu_o + \Delta\mu_{\text{ref}} + \Delta\mu_H \quad (25a)$$

where μ_o is given by eq 20b, $\Delta\mu_{\text{ref}}$ follows from eq 19,

$$\beta\Delta\mu_{\text{ref}} = \frac{\pi d_A \rho_B}{2} \int_0^1 d\lambda (d_B + \lambda d_A)^2 g_{AB}^{(\lambda)} \left(\frac{d_B + \lambda d_A}{2} \right) \quad (25b)$$

and $\Delta\mu_H$ is obtained from differentiation of eq 23 with respect to ρ_A in the zero solute concentration limit.

$$\beta\Delta\mu_H = 4\pi\rho_B \int_{\sigma_{AB}}^\infty r^2 \beta w_{AB} g_{AB}^0 dr \quad (25c)$$

In writing eq 25c we have neglected the dependence of the polymer/polymer radial distribution function on ρ_A at low concentrations of A.

At equilibrium, we can equate the chemical potential of component A in the gas and polymer phases at constant pressure and temperature.

$$\beta\mu_{\text{ig}} = \beta\mu_A^p$$

$$\ln(\beta P \Lambda^3) = \ln[\rho_A \Lambda^3 / (1 - \eta)] + \beta\Delta\mu_{\text{ref}} + \beta\Delta\mu_H \quad (26)$$

At low concentration of solute A we can write

$$\phi_A = \frac{\rho_A}{\rho_A + \rho_B} \cong \frac{\rho_A}{\rho_B} \quad (27)$$

From eqs 3, 25, and 26, we can then identify a microscopic description of the Henry's constant K_H

$$K_H = \frac{\rho_B k_B T}{(1 - \eta)} \exp(\beta\Delta\mu_{\text{ref}} + \beta\Delta\mu_H) \quad (28)$$

Unlike the Flory–Huggins result in eq 4, eq 28 allows one to compute the effect of solute size, polymer architecture, and intermolecular potentials on the solubility of gases in polymers.

III. Results & Discussion

The methods outlined in the previous section can be used to calculate the solubility of a monatomic gas in a polymer liquid. For purposes of illustration, we will now compute the solubility of the rare gases in polyethylene as a function of temperature. The Lennard–Jones parameters for He, Ne, Ar, and Xe (site A) used in this investigation are shown in Table 1. The values were

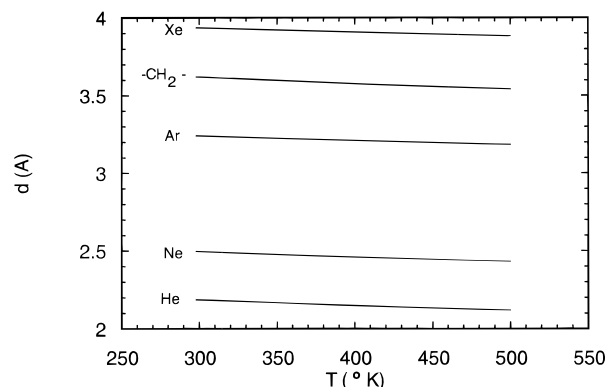


Figure 3. The effective hard-core diameters of the various sites as a function of temperature. The diameters were computed using the Barker–Henderson formalism embodied in eq 24.

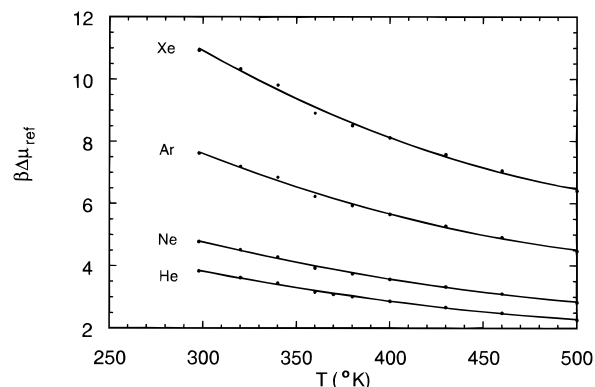


Figure 4. The athermal contribution to the solute chemical potential as a function of temperature. The points were calculated from eq 25b and the smooth curves are quadratic fits to the theory.

obtained²⁵ from second virial coefficient data in the gas phase. The corresponding parameters for a united-atom methylene site (site B) in polyethylene were taken from studies on alkanes by Jorgensen and co-workers.²⁶ The cross parameters were estimated from the Lorentz–Bertholet combining rules $\sigma_{AB} = (\sigma_A + \sigma_B)/2$ and $\epsilon_{AB} = \sqrt{\epsilon_{AA}\epsilon_{BB}}$, which should be a good approximation for sites interacting with dispersive interactions. The density of the polymer as a function of temperature was calculated from a thermal expansion coefficient (0.00085/K) determined from P , V , T data on polyethylene in the melt by Olabisi and Simha.²⁷

The optimum hard-core diameters of the sites in the athermal reference system were found as a function of temperature from eq 24. These results are shown in Figure 3. Note that the hard-core diameter decreases slightly as the temperature is increased.

Using the above parameters, together with the temperature dependent intramolecular structure functions in Figure 1, we computed the athermal chemical potential $\Delta\mu_{\text{ref}}$ from eq 25b for the series of rare gases in polyethylene. The intermolecular radial distribution function in the integrand of eq 25b was obtained for a range of hard-core diameters $(d_B + \lambda d_A)/2$ from PRISM theory as λ varies from 0 to 1. The athermal or reference chemical potential is shown in Figure 4 as a function of temperature. Note that the athermal chemical potential decreases monotonically as the temperature increases. As expected, the athermal chemical potential increases as one goes from He to Xe, since a larger expenditure of free energy is required to insert larger solute atoms.

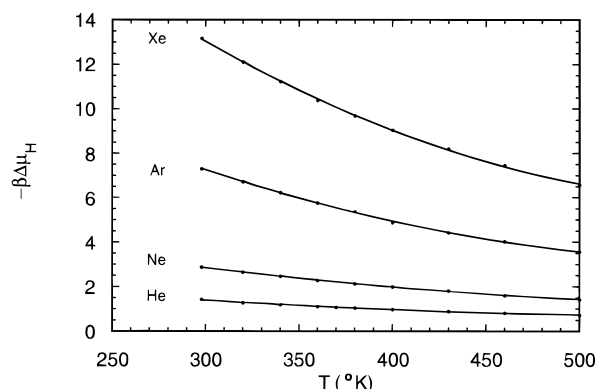


Figure 5. The enthalpic contribution to the solute chemical potential as a function of temperature. The points were calculated from eq 25c and the smooth curves are quadratic fits to the theory.

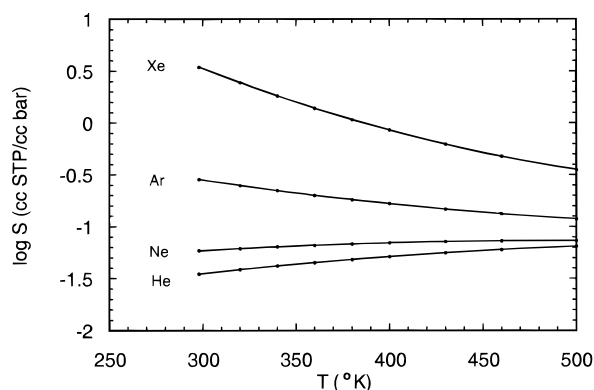


Figure 6. The solubility of the rare gases as a function of temperature calculated from PRISM theory. The points were calculated from eq 28 and the smooth curves are quadratic fits to the theory.

Since we already obtained the athermal radial distribution function $g_{AB}^0(r)$ from PRISM theory in order to evaluate the athermal chemical potential, it is a simple matter to compute the enthalpic chemical potential from eq 25c. These results are depicted in Figure 5 for the potential parameters given in Table 1. Note that the enthalpic contribution to the chemical potential is negative, thus opposing the athermal contribution. In contrast to the athermal contribution, the enthalpic chemical potential becomes more negative in going from He to Xe due to the fact that the attractive potential well deepens for the larger solute species. Furthermore, the magnitude $\Delta\mu_H$ decreases monotonically with temperature since both polymer density and $\beta\epsilon_{AB}$ decrease.

Henry's law constants can now be obtained from eq 28. In order to facilitate comparison with experiment, we will show calculations for the solubility $S = P/K_H$ at a pressure of 1 bar. These results are displayed in Figure 6. In eq 28 numerical uncertainties in $\Delta\mu_H$ and $\Delta\mu_{ref}$ are magnified because their sum appears in the exponent. In order to mitigate this effect, we evaluated the exponent in eq 28 from separate quadratic fits to the chemical potential contributions in Figures 4 and 5.

The solubility curves in Figure 6 depict several interesting features. It can be observed that gas solubility increases as the size of the solute atom increases. At first glance this may seem counterintuitive since one might naively expect that more of the smaller solute atoms could fit into the available free volume of the polymer. As can be observed in Table 1, however, the depth of the Lennard–Jones attractive well

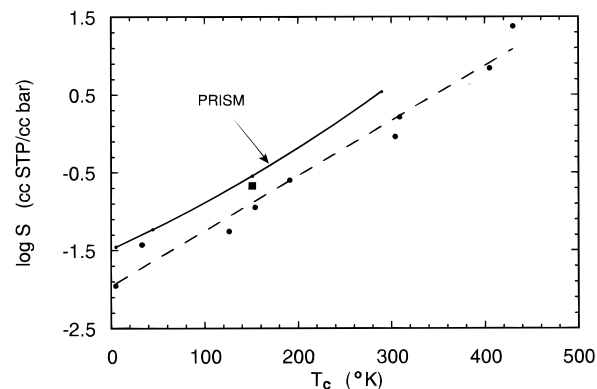


Figure 7. The solubility of various gases as a function of the critical temperature (T_c) of the solute gases. The small circles refer to the rare gas solubilities calculated from PRISM theory at 298 K; the solid curve is a quadratic fit to the theory. The large circles are experimental data at 298 K on natural rubber from ref 28. The solutes in order of increasing T_c are He, H₂, N₂, O₂, CO₂, NH₃, SO₂, CH₄, and C₂H₂. The square refers to experimental data from ref 28 for Ar in SBR rubber at 298 K.

also increases with the size of the solute. Evidently, the effect of attractions, which favor solubility, wins out over the unfavorable size effect. This trend predicted by PRISM theory is in accordance with experimental data on gas solubility in elastomers. Typically, the solubility of Ar is 10–20 times higher than He in common elastomers.²⁸

Another interesting feature of the calculations shown in Figure 6 is that the temperature coefficient of the solubility is predicted to be positive for He and Ne and negative for Ar and Xe. The temperature dependence of the solubility is a subtle effect and arises from a complex interplay of three factors: (1) the temperature dependence of the Boltzmann factor $\exp[-\beta w_{AB}(r)]$, (2) the temperature dependence of the polymer density through the thermal expansion coefficient, and (3) the temperature dependence of the intramolecular structure through the $\hat{\Omega}_{BB}(k)$ function in Figure 1. Effect 1 leads to a negative temperature coefficient, whereas effect 2 tends to increase the solubility with temperature. In the case of Ar and Xe, the dispersive interactions are large enough for effect 1 to dominate. The temperature dependence of the intramolecular structure is expected to be a small contribution. Thus effect 3 can favor a positive or negative temperature coefficient of the solubility, depending on the temperature dependence of the radius of gyration.

It has been known experimentally²⁸ for some time that light and heavy nuclei solutes have opposite temperature dependence. For example, the solubility²⁸ of He in natural rubber increases from 0.011 to 0.014 (mL STP/mL bar) as the temperature is raised from 298 to 323 K. By contrast, the solubility²⁸ of Ar decreases from 0.21 to 0.19 (mL STP/mL bar) over the same temperature range. PRISM theory is successfully able to capture this experimental trend.

It is well-known from experimental solubility measurements on a wide range of gases in elastomers^{28,29} that, for a given polymer, the solubility correlates very strongly with the critical temperature of the gas. For the case of gas solubility in natural rubber at 298 K, the following empirical correlation has been suggested²⁸

$$\log S = -2.1 + 0.0074 T_c \quad (29)$$

where the dimensions of S are (mL STP of gas/mL of

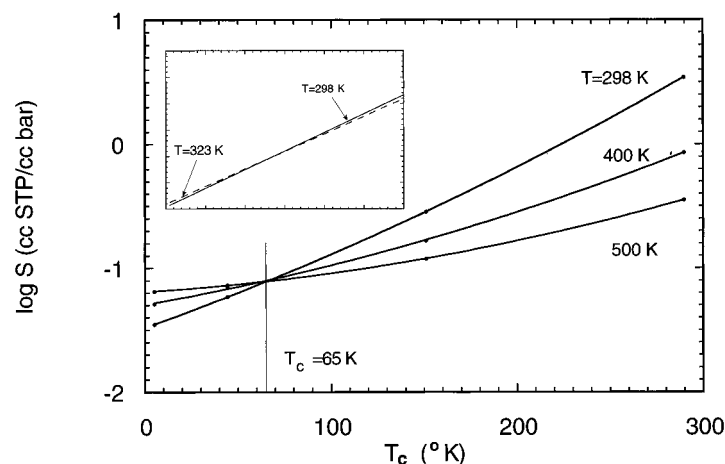


Figure 8. Solubility calculated from PRISM theory as a function of the critical temperature of the solute at the three sample temperatures indicated. The inset shows similar information at 298 and 323 K. Note that the curves appear to cross at about $T_c \approx 65$ K. This corresponds to a crossover in behavior from a positive to negative temperature coefficient of the solubility.

polymer, bar) and T_c is the critical temperature of the gas in degrees Kelvin.

To gain further insights into this correlation, we have plotted in Figure 7 the theoretical solubility as a function of the critical temperature of the gases given in Table 1. As can be seen in the figure, a smooth curve can be drawn through the four solubility points, suggesting that theory supports the empirical correlation. Also plotted in Figure 7 are experimental data at 298 K for nine different gases in natural rubber (circles) and for Ar in SBR rubber (square). The dashed line is a least square fit of the natural rubber data similar to eq 29. It can be seen from the figure that PRISM theory not only predicts the correct trends with critical temperature but also yields actual solubility values having the right order of magnitude. It is worth mentioning that the Lorentz–Bertholet approximation $\epsilon_{AB} = \sqrt{\epsilon_{AA}\epsilon_{BB}}$ was used to estimate the attractive interactions between polymer and solute. Experiment suggests,³⁰ however, that this approximation probably overestimates ϵ_{AB} by about 3–15%. Lowering of the solute–polymer interactions would lead to even better agreement between theory and experiment in Figure 7.

The information plotted in Figure 7 pertains to 298 K. Since we have seen that the solubility is temperature dependent, correlations of the type given in eq 29 would also be expected to change with the temperature of the polymer. In Figure 8 we have plotted the solubility as a function of critical temperature of the solute for various temperatures of the system. It can be seen that the curves have a similar shape, but the dependence of solubility on T_c is predicted to diminish as the sample temperature increases. Interestingly, the theoretical curves seem to cross at a single value of the critical temperature $T_c \approx 65$ K. Thus PRISM theory suggests a crossover in temperature behavior at this value. Solute gases with critical temperatures below about 65 K would be expected to have a positive temperature coefficient, whereas above this solute critical temperature the converse would be predicted. In the immediate region of this crossover critical temperature, the solubility would be expected to be temperature independent. Experimental solubility data for the solubility of various gases in natural rubber tabulated in Table 3 of ref 28 suggests that such a crossover from positive to negative temperature coefficient of solubility occurs between N_2 ($T_c = 126$ K) and O_2 ($T_c = 154$ K).

IV. Concluding Remarks

In this investigation we have applied PRISM theory to the problem of calculating the solubility of gases in polymer liquids. Using PRISM theory to compute the correlations between solute and polymer, eqs 25 and 28 provide a convenient route to the equilibrium solubility and Henry's law constants. For illustration purposes, we have carried out solubility calculations for monatomic gases in polyethylene melts. Remarkably, PRISM theory seems to capture many qualitative features of the solubility observed experimentally in common elastomeric polymers without any adjustable parameters.

The formalism presented here can be generalized to nonspherical solutes in polymers with more complex structure than polyethylene. Of considerable practical interest is the solubility of diatomic gases. An interesting question is, how important is the nonspherical geometry of a gas molecule such as N_2 or O_2 in determining the chemical potential? Although no results are shown here, we have performed preliminary calculations on the solubility of N_2 and O_2 in polyethylene by approximating the molecules as spherical sites. Reasonable and consistent results were found. More exact calculations on diatomic gases, where two sites are used to represent the molecular structure of the solute, will be the subject of future investigations.

A related application of PRISM theory is to consider the solubility of a void or cavity particle⁸ in a polymer liquid. A cavity particle interacts with the liquid like an ordinary solute molecule, but has a zero interaction potential with other cavity particles.⁸ From the chemical potential of the cavity particle as a function of the particle diameter, a measure of the free volume distribution of the polymer liquid in question can be deduced.³⁰ Hence, PRISM theory could be employed to probe the free volume distribution of various polymers as a function of chain architecture and backbone stiffness. Such an analysis could provide routes to other physical properties of interest.

Finally, it should be pointed out that computer simulation methods can also be employed to model the solubility of low molecular weight solutes in polymers.³² This can be accomplished by using particle insertion methods to compute the chemical potential of a solute in a polymer matrix. Very recently, Guillot and Guisani³³ performed molecular dynamics simulations on SiO_2 . From particle insertion methods on MD struc-

tures, these investigators estimated the solubility of the rare gases in silica over a wide range of temperature and pressure. Interestingly, the solubility of the rare gases in both glassy and liquid SiO₂ decreases with the size of the solute, in contrast to the solubility behavior of elastomeric polymers. Thus we observe that solubility of gases in polymers is a nonuniversal phenomena which depends on the details of the local packing.

Acknowledgment. The authors would like to thank David Chandler for helpful comments regarding calculation of the chemical potential of solute molecules. The authors would also like to thank the reviewer for pointing out the effect of the Lorentz–Bertholet approximation on the solubility.

References and Notes

- (1) Clough, R. L.; Gillen, K. T. *Polym. Degrad. Stabil.* **1992**, *38*, 47.
- (2) Fleming, G. K.; Koros, W. J. *Macromolecules* **1986**, *19*, 2285.
- (3) Koros, W. J.; Paul, D. R. *J. Polym. Sci., Polym. Phys.* **1978**, *16*, 1947. Chiou, J. S.; Maeda, Y.; Paul, D. R. *J. Appl. Polym. Sci.* **1985**, *30*, 4019.
- (4) Flory, P. J. *Principles of Polymer Chemistry*; Cornell University Press: Ithaca, NY, 1953.
- (5) Schweizer, K. S.; Curro, J. G. *Adv. Polym. Sci.* **1994**, *116*, 321.
- (6) Schweizer, K. S.; Curro, J. G. *Adv. Chem. Phys.* **1996**, in press.
- (7) Chandler, D.; Andersen, H. C. *J. Chem. Phys.* **1972**, *57*, 1930.
- (8) Chandler, D. in *Studies in Statistical Mechanics VIII*; Montroll, E. W., Lebowitz, J. L., Eds.; North-Holland: Amsterdam, 1982; p 274.
- (9) Pratt, L. R.; Chandler, D. *J. Chem. Phys.* **1977**, *67*, 3683.
- (10) Brandrup, J.; Immergut, E. H., Eds. *Polymer Handbook*, 3rd ed.; John Wiley & Sons: New York, 1989.
- (11) Schweizer, K. S.; Curro, J. G. *Phys. Rev. Lett.* **1987**, *58*, 246.
- (12) Curro, J. G.; Schweizer, K. S. *Macromolecules* **1987**, *20*, 1928.
- (13) Schweizer, K. S.; Curro, J. G. *Macromolecules* **1988**, *21*, 3070.
- (14) Curro, J. G. *Macromolecules* **1994**, *27*, 4665.
- (15) Schweizer, K. S.; Curro, J. G. *Phys. Rev. Lett.* **1988**, *60*, 809.
- (16) Schweizer, K. S.; Curro, J. G. *J. Chem. Phys.* **1989**, *91*, 5059.
- (17) Curro, J. G.; Schweizer, K. S. *J. Chem. Phys.* **1988**, *88*, 7242.
- (18) Curro, J. G.; Schweizer, K. S. *Macromolecules* **1991**, *24*, 6736.
- (19) Honnell, K. G.; McCoy, J. D.; Curro, J. G.; Schweizer, K. S.; Narten, A. H.; Habenschuss, A. *J. Chem. Phys.* **1991**, *94*, 4659.
- (20) Narten, A. H.; Habenschuss, A.; Honnell, K. G.; McCoy, J. D.; Curro, J. G.; Schweizer, K. S. *J. Chem. Soc., Faraday Trans.* **1992**, *88*, 1791.
- (21) Rajasekaran, J. J.; Curro, J. G.; Honeycutt, J. D. *Macromolecules* **1995**, *28*, 6843.
- (22) Hansen, J. P.; McDonald, I. R. *Theory of Simple Liquids*; Academic Press: London, 1986.
- (23) McCoy, J. D.; Honnell, K. G.; Curro, J. G.; Schweizer, K. S.; Honeycutt, J. D. *Macromolecules* **1992**, *25*, 4905.
- (24) Barker, J. A.; Henderson, D. *Ann. Rev. Phys. Chem.* **1972**, *23*, 439.
- (25) Hirschfelder, J. O.; Curtis, C. F.; Byrd, R. B. *Molecular Theory of Gases and Liquids*; John Wiley & Sons: New York, 1954.
- (26) Jorgensen, W. L.; Madura, J. D.; Swenson, C. J. *J. Am. Chem. Soc.* **1984**, *106*, 6638.
- (27) Olabisi, O.; Simha, R. *Macromolecules* **1975**, *8*, 206.
- (28) Van Amerongen, G. J. *Rubber Chem., & Tech.* **1964**, *37*, 1065.
- (29) Van Krevelen, D. W.; Hoftyzer, P. J. *Properties of Polymers: Their Estimation and Correlation with Chemical Structure*; Elsevier: Amsterdam, 1976.
- (30) See Table 8.4–17 in ref 25. The authors are indebted to the reviewer for pointing this out.
- (31) Honnell, K. G.; Curro, J. G. *Macromolecules*, in preparation.
- (32) See, for example: de Pablo, J. J.; Laso, M.; Suter, U. W. *Macromolecules* **1993**, *26*, 6180.
- (33) Guillot, B.; Guissani, Y. *J. Chem. Phys.* **1996**, *105*, 255.

MA961084S